Published in final edited form as:

IEEE J Sel Top Quantum Electron. 2007 ; 13(6): 1715–1720. doi:10.1109/jstqe.2007.910804.

In Vivo Detection of Gold Nanoshells in Tumors Using Diffuse Optical Spectroscopy

Raiyan T. Zaman,
Department of Biomedical Engineering, University of Texas at Austin, Austin, TX 78712 USA

Parmeswaran Diagaradjane
Radiation Oncology, MD Anderson Cancer Center, Houston, TX 77030-4090 USA

James C. Wang, **Jon Schwartz**
Nanospectra Biosciences, Inc., Houston, TX 77054 USA

Narasimhan Rajaram,
Department of Biomedical Engineering, University of Texas at Austin, Austin, TX 78712 USA

Kelly L. Gill-Sharp,
Nanospectra Biosciences, Inc., Houston, TX 77054 USA

Sang H. Cho,
MD Anderson Cancer Center, University of Texas, Houston, TX 77030 USA. He is now with the Department of Mechanical Engineering, Georgia Institute of Technology, Atlanta, GA 30332 USA

Henry Grady Rylander III [Member, IEEE],
Department of Biomedical Engineering, University of Texas at Austin, Austin, TX 78712 USA

J. Donald Payne,
Nanospectra Biosciences, Inc., Houston, TX 77054 USA

Sunil Krishnan,
Radiation Oncology, MD Anderson Cancer Center, Houston, TX 77030-4090 USA

James W. Tunnell [Member, IEEE]
Department of Biomedical Engineering, University of Texas at Austin, Austin, TX 78712 USA

Abstract

This study demonstrates the use of diffuse optical spectroscopy (DOS) for the noninvasive measurement of gold nanoshell concentrations in tumors of live mice. We measured the diffuse optical spectra (500–800 nm) using an optical fiber probe placed in contact with the tissue surface. We performed *in vitro* studies on tissue phantoms illustrating an accurate measurement of gold–silica nanoshell concentration within 12.6% of the known concentration. *In vivo* studies were performed on a mouse xenograft tumor model. DOS spectra were measured at preinjection, immediately postinjection, 1 and 24 h postinjection times, and the nanoshell concentrations were verified using neutron activation analysis.

raiyan_zaman@yahoo.com.

Index Terms —

Contrast agents; diffuse optical spectroscopy (DOS); diffusion theory; gold nanoparticles; optical imaging

I. Introduction

GOLD nanoshells have recently been demonstrated for use in a new type of laser-induced thermal therapy of tumors [1], [2] and cancerous cell lines [3]. Gold nanoshells are biologically inert and optically tunable nanoparticles composed of silica cores coated with an ultrathin gold layer [4]. The optical properties can be tuned by varying the relative size of the core and the thickness of the shell. In particular, these particles can be designed to absorb near-infrared light, and when irradiated by a laser, provide an exogenous vehicle to convert optical energy into heat. In addition, the particles passively extravasate through the leaky and aberrant blood vessels within tumors, a process known as the enhanced permeability and retention (EPR) effect [5]. Thus, intravenous administration of gold nanoshells leads to nanoparticle accumulation within the tumor, and the illumination of these areas with near-infrared light leads to hyperthermia [2].

The optimum lethal dose is achieved when nanoparticles accumulate with maximum affinity to the tumor site. While targeting of macromolecular anticancer drugs has been studied in great detail, less is known about the dynamics of EPR for metal nanoparticles *in vivo* primarily due to the lack of techniques to noninvasively monitor them in a tissue. For example, the current standard method to measure gold nanoshell concentrations in tissue is neutron activation analysis (NAA) [6]. This method requires tissue excision, dehydration, and irradiation within a nuclear reactor. While extremely sensitive, this method is invasive, and thus, does not allow for longitudinal monitoring of metal nanoparticles in living systems.

Therefore, we have developed a noninvasive optical technique [diffuse optical spectroscopy (DOS)] for monitoring gold nanoshell concentrations in bulk tissue. The goal of this study was to demonstrate the use of DOS to measure gold nanoshell concentration in tumors of live mice. Our approach involved the testing of the optical spectroscopic system *in vitro* (tissue phantoms) and *in vivo* (small animal model).

Various DOS measurements have been used *in vivo* to quantify the hemoglobin concentration and blood oxygen saturation, the amount of scattering (i.e., the reduced scattering coefficient), water content, and melanin [7]–[9]. As nanoshells are optical devices with specific reflectance spectra [10], DOS also enables *in vivo* measurement of gold nanoshell concentrations. In DOS, light is delivered to and collected from tissue via an optical fiber probe, allowing specificity of the area interrogated as well as ease of use.

II. Materials and Methods

A. DOS System

Fig. 1 illustrates the DOS system consisting of three main components: light source (LS-1 Tungsten Halogen lamp, Ocean Optics), optical fiber probe (custom built prototype), and spectrometer (USB4000, Ocean Optics). The tungsten halogen lamp was connected to the optical probe through a Subminiature version A (SMA) connector. The sample was illuminated with one optical fiber (the source fiber), and the reflected light was collected with a separate optical fiber (the detector fiber) that was 2.15 mm from the source fiber. The detector fiber was coupled to the spectrometer, and the reflectance spectrum was collected over a wavelength range of 500–800 nm. Each reflectance spectrum was collected in a fraction of a second. Prior to spectral analysis, recorded signals were corrected for system response. We subtracted the detector dark current and normalized the sample reflectance by the reflectance of a Lambertian reflector (Spectralon, Labsphere, Inc.; 20% reflector).

B. Diffusion Model

We measured diffuse reflectance using an optical fiber probe with the geometry described before. The source fiber delivers light to the tissue surface where the light enters the tissue and undergoes multiple scattering events. Part of this light is absorbed, while the remaining light exits the tissue surface as diffuse reflectance. The detector fiber, also in contact with the tissue surface, collects part of this emerging diffuse reflectance, while light not incident on the detector fiber exits the tissue undetected. The collected diffuse reflectance depends on the tissue optical properties and the geometry of the optical fiber probe.

To model the diffuse reflectance, we employed the steady-state spatially resolved diffusion approximation described by Farrell *et al.* [11]. This model describes the diffuse reflectance at a distance r from the point of incidence as a function of two parameters: the reduced scattering coefficient $\mu'_s(\lambda)$ and the absorption coefficient $\mu_a(\lambda)$ (λ is the wavelength of light). Assuming a narrow beam of light incident on the surface of a semi-infinite medium, Farrell *et al.* obtained the following analytical solution for the diffuse reflectance in the diffusion approximation [11]:

$$R(\lambda, r) = \frac{z_0}{4\pi}\frac{\mu'_s}{\mu'_s + \mu_a}\left[\left(\mu + \frac{1}{r_1}\right)\frac{\exp(-\mu r_1)}{r_1^2} + \left(1 + \frac{4}{3}A\right)\left(\mu + \frac{1}{r_2}\right)\frac{\exp(-\mu r_2)}{r_2^2}\right] \quad (1)$$

where

$$\mu = [3\mu_a(\mu_a + \mu'_s)]^{1/2}$$
$$z_0 = \frac{1}{\mu_a + \mu'_s}$$
$$r_1 = \left(z_0^2 + r^2\right)^{1/2}$$
$$r_2 = \left[z_0^2\left(1 + \frac{4}{3}A\right)^2 + r^2\right]^{1/2}.$$

The parameter A depends on the refractive index of the medium and is assumed to be 3.2 for the tissue [11]. This model assumes the biological tissue to have homogeneous optical

properties. Therefore, optical properties represent volumetric averages over the sampling volume of the probe.

We constrained the reduced scattering coefficient to the following form:

$$\mu'_s(\lambda) = \mu'_s(\lambda_0)\left(\frac{\lambda}{\lambda_0}\right)^{-B} \quad (2)$$

where λ is the wavelength in nanometers, λ_0 = 630 nm, and B is the power law slope that is related to the average size of scatterers [12].

We assumed that absorption within the 500–800 nm spectral region was due only to oxy- and deoxy-hemoglobin and gold nanoshells. Therefore, we expressed the absorption coefficient μ_a as a linear combination of the nanoshell and blood absorption coefficients, $\mu_{a,\mathrm{NS}}$ and $\mu_{\mathrm{a,Blood}}$, respectively:

$$\mu_a = \mu_{\mathrm{a,NS}} + \mu_{\mathrm{a,Blood}} = c_{\mathrm{NS}}\sigma_{\mathrm{NS}} + c_{\mathrm{Hb}}\left(\alpha\sigma_{\mathrm{HbO_2}} + (1-\alpha)\sigma_{\mathrm{Hb}}\right) \quad (3)$$

where c_{NS} is the nanoshell concentration, c_{Hb} is the total hemoglobin (Hb) concentration, σ_{NS} is the nanoshell absorption cross section, α is the O_2 saturation, $\sigma_{\mathrm{HbO_2}}$ is the absorption cross section of oxygenated Hb, and σ_{Hb} is the absorption cross section of deoxygenated Hb. We applied a nonlinear constrained optimization fitting algorithm (Optimization Toolbox, MatLab, Mathworks) to extract five fit parameters: c_{Hb}, c_{NS}, α, B, and $\mu'_s(\lambda_0)$. The constraints for the fit parameters were chosen to include the expected physiologically relevant range (c_{Hb} : 0–25.0; c_{NS} : 0–3 × 10^9; α : 0–1.0; B : 0–2; $\mu'_s(\lambda_0)$: 0.5 – 25.0.

C. Tissue Phantoms

The goal of the tissue phantom study was to determine the accuracy of DOS to detect gold nanoshells under physiologically relevant values of scattering and absorption. Tissue phantoms allowed for a controlled system with *a priori* knowledge of the quantities of scatters and absorbers. The tissue phantoms were fabricated from 10% intralipid $\left(\mu'_s = 1\,\mathrm{mm}^{-1}\right)$, without and with (3 mg/mL) Hb and varying nanoshell concentrations (1.03 × 10^8–15.4 × 10^8 particle/mL) obtained from Nanospectra Biosciences, Inc. These “known” nanoshell concentrations are estimated to be within 20% of the actual concentration and represent the physiological range shown to accumulate in murine tumors [6], [13].

D. Gold–Silica Nanoshells

Gold–silica nanoshells were synthesized using the seed-mediated method. Colloidal silica (120 nm diameter) was used as the core of the particle (Precision Colloids). Very small gold colloid (1–3 nm) was grown by using the method of Duff *et al.* [14]. This colloid was aged for 2 weeks at 4 ℃. Aminated silica particles were then added to the gold colloid suspension [15]. Gold colloid adsorbs to the amine groups on the silica surface, resulting in a silica particle covered with gold colloid as nucleating sites. Gold–silica nanoshells were then grown by reacting $HAuCl_4$ with the silica–colloid particles in the presence of formaldehyde. This process reduces additional gold onto the adsorbed colloid, which act as nucleation sites,

causing the surface colloid to grow and coalesce with neighboring colloid, forming a complete metal shell. Particle formation was assessed using a UV–Vis spectrophotometer. Fig. 2 illustrates the extinction spectrum of the particles used in this study. Particles for this study were designed to have a 120-nm-core-diameter and a 14-nm-thick shell resulting in an absorption peak between 780 and 800 nm. For passive targeting, a Thiolated Polyethylene glycol (SH-PEG) (Laysan Bio, Huntsville, AL) is assembled onto nanoshell surfaces by combining 5 μM SH-PEG and 1.5×10^{10} particles/mL in deionized water (3.2×10^5 SH-PEG molecules/particle) for 12 h, followed by diafiltration to remove the excess SH-PEG. Before injection, nanoshells were suspended in 10% trehalose solution to create an isosmotic solution for injection.

E. Animal Model

The goal of the animal model was to demonstrate the feasibility of an *in vivo* quantification of nanoshells using DOS. Six-to eight-week-old Swiss athymic mice ($n = 7$) were subcutaneously injected with rat C6-glioma cells (1×10^6cells/μL) on the right flank. Tumor growth was monitored until the tumor diameters reached approximately 1 cm. All mice were systemically administered nanoshells through the tail vein.

Preinjection DOS measurements were acquired from the tumor sites of all the animals prior to the injection (tail vein) of nanoshells (8×10^8 nanoshells/g), and the subsequent DOS were measured immediately postinjection, and at 1 and 24 h postinjection times. The distal end of the optical fiber probe was placed in gentle contact with the skin surface near the center of the tumor site. The nanoshell concentrations were estimated as in the tissue phantoms. The DOS estimated nanoshell concentrations were compared with NAA of the tissue samples extracted at the time points mentioned earlier. NAA is the “gold standard” method for trace gold quantification in biological samples, with sensitivities down to 70 pg [6]. NAA requires extraction of the whole tumor-containing gold nanoshells for accurate measurement. The tissues were dehydrated completely before irradiating them inside the reactor. The concentrations of nanoshells were calculated based on the half-life of the metal particles according to James *et al.* [6].

III. Results and Discussion

A. Tissue Phantoms

Fig. 3(a) illustrates the reflectance of tissue phantoms with Hb and various concentrations of nanoshells. The dips in the reflectance at 540 and 570 nm are due to the absorption by the *Q*-bands of Hb [16], [17]. The phantom without nanoshells resulted in the highest overall reflectance spectrum. As the nanoshell concentration increased, the measured reflectance spectra decreased monotonically. This trend was also observed in the tissue phantoms without Hb (data not shown).

Experimental reflectance data were fit with the diffusion model to determine the measured concentrations of the metal nanoshells in the tissue phantoms. The measured versus known nanoshell concentrations are illustrated in Fig. 3(b). Also plotted is the “45°” line to represent the ideal relationship between the measured and known concentrations. These

functions demonstrate the ability of DOS to extract nanoshell concentrations within the physiologically relevant range. The error in estimating nanoshell concentrations in tissue phantoms was between 0.05–12.6% and 3.0–10.3% with and without Hb, respectively. The error in estimating Hb concentrations and O_2 saturations in these tissue phantoms varied from 15.8% to 37.5% and 21.1% to 47.3%, respectively. Our current algorithm prioritized the weighting for fitting nanoshell concentration over the other fit parameters. The errors in estimating the Hb concentrations and O_2 saturations may be improved through further development of the inverse algorithm.

The detection range of the nanoshell concentration in tissue depends on the distance between the source and detector fibers. The sampled optical path length increases as the source–detector distance increases, and thus, the upper concentration limit can be adjusted. For our experiment with a source detector separation of 2.15 mm, we were able to detect concentrations up to 15.4×10^8 particles/mL. This upper limit could be increased by moving the source and detector fibers closer.

B. Animal Model

Fig. 4(a) illustrates the reflectance measurements from a tumor site at the four time points for a single animal. The reflectance of the preinjection measurement had the highest overall reflectance with the immediately postinjection reflectance measurement slightly less. However, for this animal, the 1 h reflectance measurement had the lowest reflectance intensity while the 24 h reflectance was slightly higher. These large changes in the diffuse reflectance, especially in the near infrared region, indicate the sensitivity of DOS to measure dynamic changes in tumor nanoshell concentrations over time.

The corresponding *in vivo* measured nanoparticle concentrations are shown in Fig. 4(b) with the highest concentration of nanoshells occurring at 1 h postinjection. Previous biodistribution studies have shown that nanoshells have a circulatory half life just under 4 h [6]. As DOS samples nanoshells in both the blood and the tumor, the decrease in nanoshells observed from 1 to 24 h is most likely due to nanoshell clearance from the blood. These data demonstrate the dynamic nature of nanoshell accumulation within the tumor site of a single animal.

Fig. 5 illustrates the correlation between the NAA and DOS methods for measuring nanoshell concentration for all specimens ($n = 7$). The tumor tissue samples from three murine specimens were collected 1 h after the nanoshell injection, and subsequently, processed for NAA. The tumor tissue samples were collected from the rest of the four murine specimens at 24 h after the nanoshell injection, and subsequently, processed for NAA. The differences between the DOS and NAA methods for measuring the 1 and 24 h post-IV-injection nanoshell concentrations were between 0.6%–7.0% and 1.5%–20.3%, respectively. We note that generally DOS agreed with NAA within 10% with the exception of one specimen, as indicated in Fig. 5. This agreement between NAA and DOS indicates the highly sensitive nature of DOS for measuring nanoshell concentrations in tissue. While NAA requires several weeks for tissue processing, DOS provides immediate results.

These data also demonstrate considerable overlap in the nanoshell accumulation in the tumor between the 1 and 24 h time points. It has been shown in the past using NAA that shells accumulate steadily for 12–24 h [6]. The large overlap shown in our data may be the result of varying tumor sizes, errors in Intravenous (IV) injection efficiencies, or potentially large amounts of nanoshell-doped blood in the tissue samples. Nevertheless, the DOS measurements shown here agree well with the standard NAA method.

IV. Conclusion

These *in vitro* and *in vivo* studies demonstrate the sensitivity of DOS to measure nanoshell concentrations within the tissue phantoms and tumors of live mice. Tissue phantom measurements demonstrated the ability of DOS to extract nanoshell concentrations within the physiologically relevant range. The accuracy of the DOS measurement in the tissue phantom was within 12.6%. *In vivo* measurements demonstrated the sensitivity of DOS to detect nanoshells present within the tumor at each of the time points, and these results agreed with NAA within 20.3%. Both NAA and DOS measured nanoshell concentrations revealed that nanoshell dosages were largely varied from specimen to specimen.

DOS represents a technique capable of real-time accurate determination of tissue nanoparticle concentrations. While the spectra in this study were analyzed offline, DOS is easily adaptable to a real-time analysis system. The total time for data collection was a fraction of a second, and spectral fitting required less than a second as well. Therefore, one could utilize DOS to monitor tumor nanoparticle concentrations longitudinally.

DOS opens new possibilities for studying the dynamics of nanoparticle accumulation in tissue, for determining relative accumulation rates for active antibody-mediated targeting versus passive EPR, and the effect of particle size and shape on ultimate biodistribution. While these experiments were carried out using gold nanoshells, this method can be extended to other metal nanoparticles such as gold nanospheres and nanorods. In addition, because DOS measures tissue physiology (i.e., blood content and O_2 saturation), it can be used to simultaneously monitor tumor physiology and treatment response during photothermal therapy.

Acknowledgments

This work was supported in part by the Charles W. & Judy Spence Tate Foundation.

Biographies

Raiyan T. Zaman received the B.Sc. degree in electrical engineering from the University of Texas at Austin, Austin, in 2000, and the Master degree *in vivo* detection of gold nanoparticles in tumors using diffuse optical spectroscopy. From the University of Texas at Austin, in 2006. She is currently working toward the Ph.D. degree in biomedical engineering track in the Electrical and Computer Engineering Department, University of Texas at Austin, Austin.

She was a Senior Applications Engineer at Motorola for five years. Her current research interests include laser tissue interaction and enhancement of light in tissue using hyper-osmotic agents.

Parmeswaran Diagaradjane received the B.S. degree in physics from Madras University, Chennai, India, in 1992, and the M.S. and Ph.D. degrees in medical physics from Anna University, Chennai, in 1994 and 2003, respectively.

He was a Postdoctoral Research Associate in the Bioengineering Department, Rice University, Houston, TX. He was a Visiting Scholar at the Oregon Medical Laser Center, Portland, and the Laser-Forshungslabor, Klinikum Großhadern, Ludwig-Maximilians-Universität München, München, Germany, in 1999 and 2001, respectively. He is currently a Research Scientist in the Department of Radiation Oncology, MD Anderson Cancer Center, University of Texas, Houston. His current research interests include nano-biophotonics, molecular imaging of tumor markers, radiosensitization, photodynamic therapy, photothermal therapy, fluorescence/optical diagnosis, and bioluminescence imaging.

He is a member of the American Society for Lasers in Medicine and Surgery, the American Society of Photodynamic Therapy, the Association of Medical Physicists of India, and the Indian Laser Association.

James C. Wang received the B.S. degree in biomedical engineering from the University of Rochester, Rochester, NY, in 2005.

He is currently a Research Engineer at the Nanospectra Biosciences, Inc., Houston, TX. He is also a Visiting Scientist in the Department of Experimental Radiation Oncology, MD Anderson Cancer Center, University of Texas, Houston.

Jon Schwartz received the B.S.E.E. and M.E.E. degrees from Rice University, Houston, TX, in 1979 and 1980, respectively, and the Ph.D. degree in biophysics from the Graduate School of Biomedical Sciences, University of Texas, Houston, in 2001.

He has been engaged in electrooptics and various disciplines of bioscience. He was a Member of the Technical Staff, NASA’s Jet Propulsion Laboratory, Pasadena, CA, for six years, and a Research Engineer at the MD Anderson Cancer Center, University of Texas, in

the Laser Biology Research and the Di-electrophoresis Laboratories for 14 years. He is currently a Chief Research Scientist for Nanospectra Biosciences, Inc., Houston.

Narasimhan Rajaram received the B.Eng. degree in electronics and instrumentation from Anna University, Chennai, India, in 2005. He is currently working toward the Ph.D. degree in biomedical engineering at the University of Texas at Austin, Austin.

His current research interests include biomedical optics, optical spectroscopy, and detection of early cancer.

Kelly L. Gill-Sharp received the B.S. degree in biomedical science from Texas A&M University, College Station, in 2003.

She has worked for four years in life science applications in nanotechnology. She is currently the Animal Program Manager for Nanospectra Biosciences, Inc., Houston, TX.

Sang H. Cho received the Ph.D. degree in nuclear engineering specializing in medical physics from Texas A&M University, College Station, in 1997.

He joined the MD Anderson Cancer Center, University of Texas, Houston, as a Postdoctoral Fellow, and later, became an Associate Professor. Since January 2007, he has been an Associate Professor of medical physics within the School of Mechanical Engineering, Georgia Tech, Atlanta. His current research interests include the use of various nanoparticles, especially gold nanoparticles, for cancer therapy and detection.

Henry Grady Rylander, III (M’68) received the B.S.E.E. and M.S.E.E. degree from the University of Texas at Austin, Austin, in 1970 and 1974, respectively, and the M.D. degree from the Health Science Center, University of Texas, San Antonio, in 1974.

He was an Intern in internal medicine at the Bexar County Teaching Hospitals and an ophthalmology residency at Audie Murphy VAH. Since 1978, he has been with the University of Texas at Austin, where he is currently the W. J. Murray Professorship in the Department of Biomedical Engineering. His current research interests include medical imaging, biosensors, and medical electronics.

J. Donald Payne Photograph and biography not available at the time of punlication.

Sunil Krishnan received the M.D. degree from the Christian Medical College, Vellore, India, in 1993.

In 2000, he completed a medicine residency at Penn State Geisinger Medical Center, Danville, PA, and in 2004, a radiation oncology residency at the Mayo Clinic in Rochester, MN. During 2004, he was an Assistant Professor in the Department of Radiation Oncology, MD Anderson Cancer Center, Houston, TX. He is currently with the Department of Biomedical Engineering, University of Texas at Austin, Austin.

James W. Tunnell (M'05) received the B.S. degree in electrical and computer engineering from the University of Texas at Austin, Austin, in 1998, and the Ph.D. degree in bioengineering from Rice University, Houston, TX, in 2002.

He was a Postdoctoral Fellow in the G.R. Harrison Spectroscopy Laboratory, Massachusetts Institute of Technology, Cambridge. In 2005, he joined the Department of Biomedical Engineering, University of Texas at Austin, Austin, as an Assistant Professor.

References

[1]. Hirsch LR, Stafford RJ, Bankson JA, Sershen SR, Rivera B, Price RE, Hazle JD, Halas NJ, and West JL, "Nanoshell-mediated near-infrared thermal therapy of tumors under magnetic resonance guidance," Proc. Nat. Acad. Sci. USA, vol. 100, no. 23, pp. 13549–13554, Nov. 11, 2003. [PubMed: 14597719]

[2]. O'Neal DP, Hirsch LR, Halas NJ, Payne JD, and West JL, "Photothermal tumor ablation in mice using near infrared-absorbing nanoparticles," Cancer Lett, vol. 209, no. 2, pp. 171–176, Jun. 2004. [PubMed: 15159019]

[3]. Loo C, Lowery A, Halas N, West J, and Drezek R, "Immunotargeted nanoshells for integrated cancer imaging and therapy," Nanoletters, vol. 5, no. 4, pp. 709–711, Apr. 2005.

[4]. Oldenburg SJ, Jackson JB, Westcott SL, and Halas NJ, "Infrared extinction properties of gold nanoshells," Appl. Phys. Lett, vol. 75, no. 19, pp. 2897–2899, Nov. 1999.

[5]. Maeda H, Fang J, Inutsuka T, and Kitamoto Y, "Vascular permeability enhancement in solid tumor: Various factors, mechanisms involved and its implications," Int. Immunopharmacol, vol. 3, no. 3, pp. 319–328, Mar. 2003. [PubMed: 12639809]

[6]. James WD, Hirsch LR, West JL, O'Neal PD, and Payne JD, "Application of INAA to the build-up and clearance of gold nanoshells in clinical studies in mice," J. Radioana. Nucl. Chem, vol. 271, no. 2, pp. 455–459, Feb. 2007.

[7]. Shah N, Cerussi A, Eker C, Espinoza J, Butler J, Fishkin J, Hornung R, and Tromberg B, "Noninvasive functional optical spectroscopy of human breast tissue," Proc. Nat. Acad. Sci. USA, vol. 98, no. 8, pp. 4420–4425, Apr. 2001. [PubMed: 11287650]

[8]. Zonios G, Perelman LT, Backman VM, Manoharan R, Fitzmaurice M, Van Dam J, and Feld MS, "Diffuse reflectance spectroscopy of human adenomatous colon polyps in vivo," Appl. Opt, vol. 38, no. 31, pp. 6628–6637, Nov. 1999. [PubMed: 18324198]

[9]. Hull EL and Foster TH, "Steady-state reflectance spectroscopy in the p-3 approximation," J. Opt. Soc. Amer. A, Opt. Image Sci. Vis, vol. 18, no. 3, pp. 584–599, Mar. 2001.

[10]. Lin AWH, Lewinski NA, Lee MH, and Drezek RA, "Reflectance spectroscopy of gold nanoshells: Computational predictions and experimental measurements," J. Nanoparticle Res, vol. 8, no. 5, pp. 681–692, Oct. 2006.

[11]. Farrell TJ, Patterson MS, and Wilson B, "A diffusion-theory model of spatially resolved, steady-state diffuse reflectance for the noninvasive determination of tissue optical-properties invivo," Med. Phys, vol. 19, no. 4, pp. 879–888, Jul-Aug 1992. [PubMed: 1518476]

[12]. Mourant JR, Fuselier T, Boyer J, Johnson TM, and Bigio IJ, "Predictions and measurements of scattering and absorption over broad wavelength ranges in tissue phantoms," Appl. Opt, vol. 36, no. 4, pp. 949–957, Feb. 1997. [PubMed: 18250760]

[13]. Hirsch LR, "Diagnostic and therapeutic applications of metal nanoshells," Ph.D. dissertation, Dept. Bioeng., Rice Univ, Houston, TX, 2004.

[14]. Duff DG, Baiker A, and Edwards PP, "A new hydrosol of gold clusters.1, formation and particle-size variation," Langmuir, vol. 9, no. 9, pp. 2301–2309, Sep. 1993.

[15]. Oldenburg SJ, Averitt RD, Westcott SL, and Halas NJ, "Nano-engineering of optical resonances," Chemi. Phys. Lett, vol. 288, no. 2–4, pp. 243–247, 5 1998.

[16]. Prahl S, "Optical absorption of hemoglobin" (Oregon Medical Laser Center, Portland, Oreg, 12 15, 1999) [Online]. Available: http://omlc.ogi.edu/spectra/hemoglobin/

[17]. Takatani S and Graham MD, “Theoretical-analysis of diffuse reflectance from a 2-layer tissue model,” IEEE Trans. Biomed. Eng, vol. BME-26, no. 12, pp. 656–664, Dec. 1979.

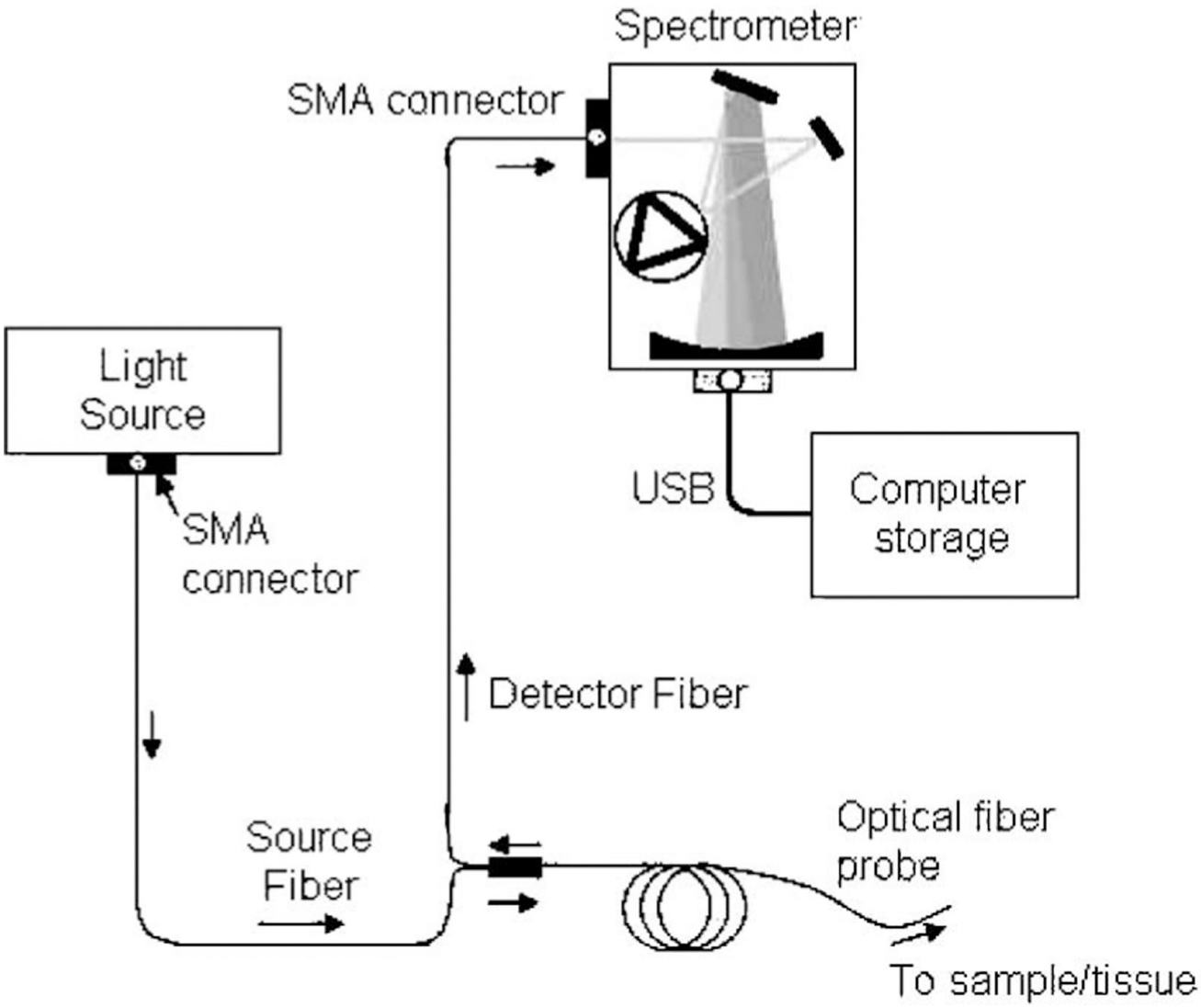

Fig. 1.
Schematic representation of the DOS system.

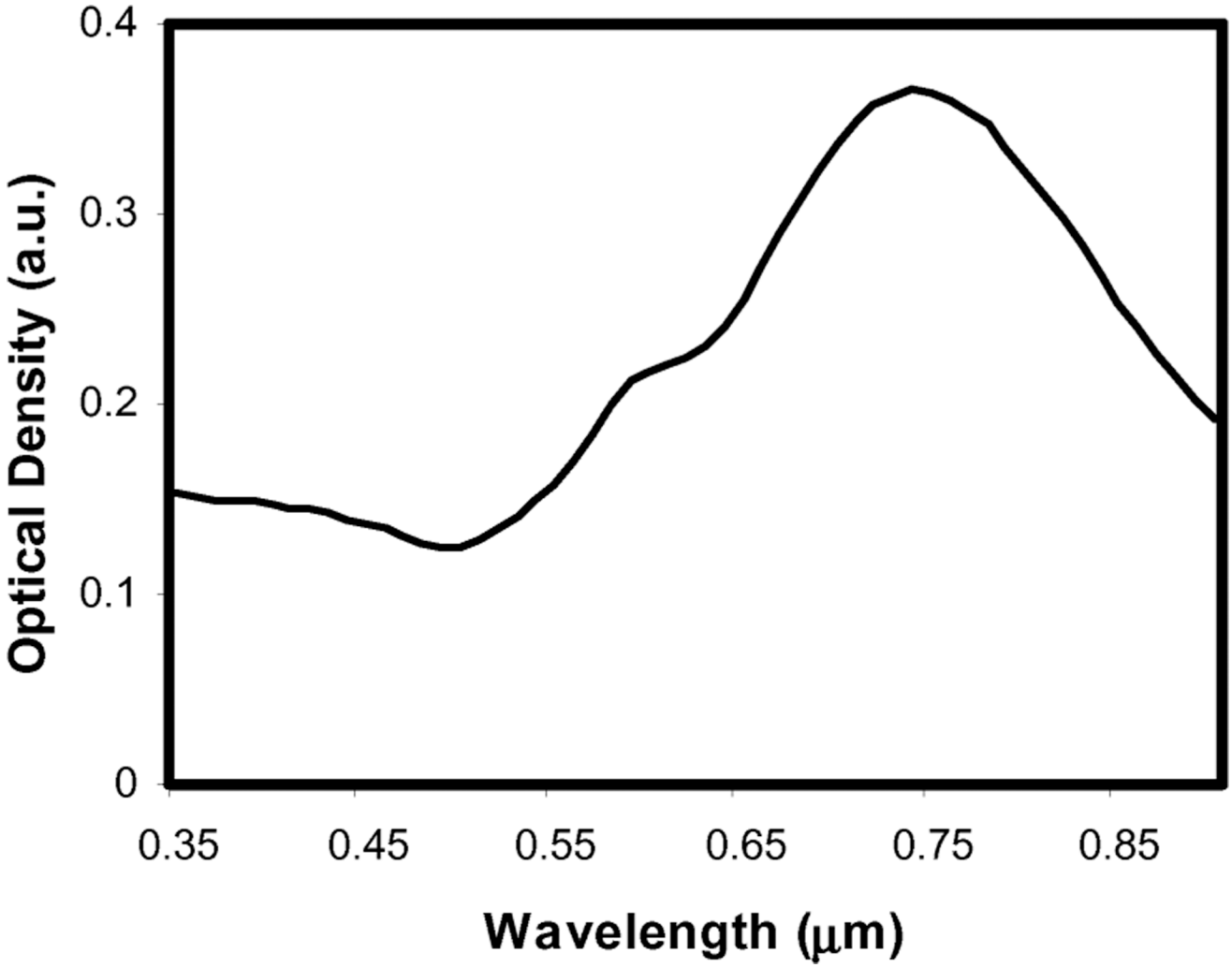

Fig. 2.
Extinction spectrum of gold/silica nanoshells used for this study. The particles had a core radius of 60 nm with a shell thickness of 14 nm.

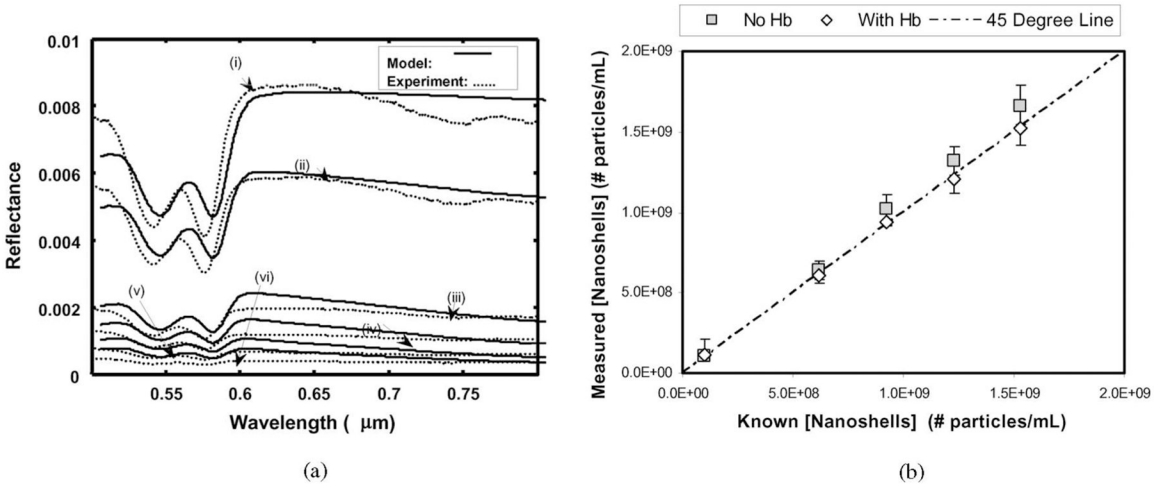

Fig. 3.

DOS measurements of gold nanoshells *in vitro*. (a) DOS reflectance spectra and diffusion theory model fits for tissue simulating phantoms with Hb and varying amounts of nanoshells. (i) no nanoshells; (ii) 1.16×10^8 particles/mL; (iii) 6.10×10^8 particles/mL; (iv) 9.42×10^8 particles/mL; (v) 12.03×10^8 particles/mL; (vi) 15.23×10^8 particles/mL. (b) DOS measured nanoshell concentrations compared to known nanoshell concentrations in tissue phantoms both with (squares) and without (diamonds) Hb. Error bars were calculated using the χ^2 goodness of fit.

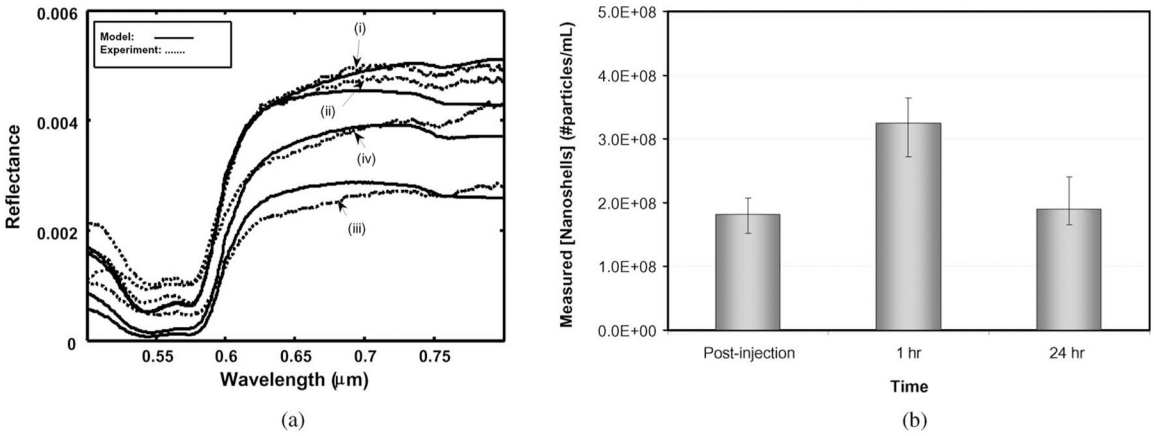

Fig. 4.

DOS measurements of gold nanoshells *in vivo*. (a) DOS reflectance spectra and diffusion theory model fits for mouse tumor with gold nanoshells at four time points: (i) preinjection; (ii) immediately postinjection; (iii) 1 h post-IV-injection; (iv) 24 h post-IV-injection. (b) *In vivo* gold nanoshell concentrations at various post-IV-injection time points. Error bars are calculated using χ^2 goodness of fit. All values are statistically significant ($p < 0.1$) (Tukey–Kramer multicomparison test).

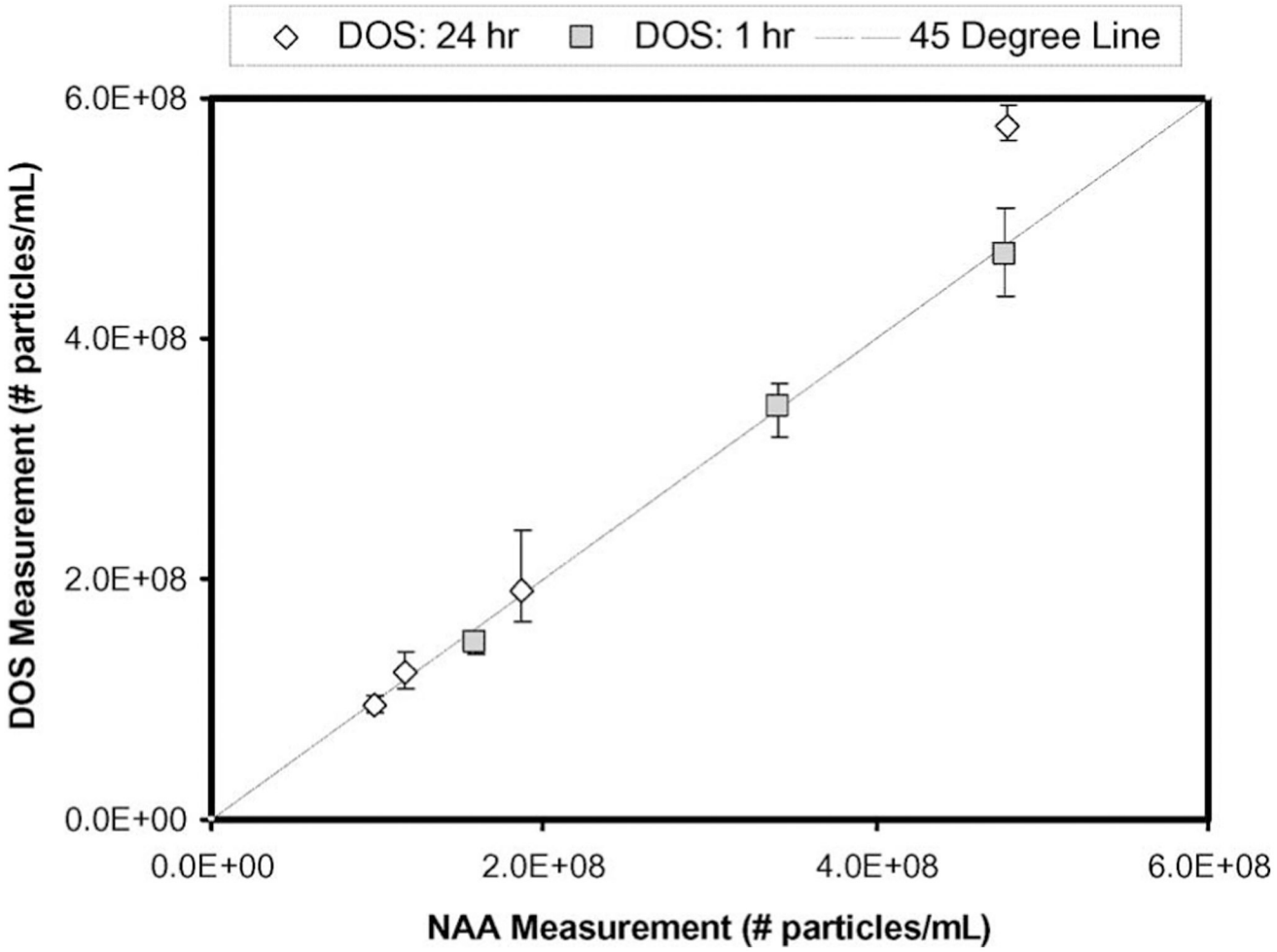

Fig. 5.

DOS versus NAA nanoshell concentrations in tumor tissue from three mice at 1 h (squares) and four mice at 24 h (diamonds) post-IV-injection of nanoshell. Error bars were calculated with χ^2 goodness of fit.